


 Cite this: *RSC Adv.*, 2021, 11, 22921

Unimodal sized silica nanocapsules produced through water-in-oil emulsions prepared by sequential irradiation of kilo- and submega-hertz ultrasounds†

 Takahiro Nemoto,^a Toshio Sakai^a and Tomohiko Okada *^{ab}

This study investigates the regulation of the size of 100 nm hollow-sphere silica particles using surfactant-free water-in-oil (W/O) emulsion. First, water droplets were dispersed in soybean oil *via* sequential ultrasound irradiation (28 kHz → 200 kHz → 950 kHz). A precursor of hollow silica particles was prepared using hydrolysis and polymerization of methylsilyl trichloride into a stable W/O emulsion. The final structure/morphology of the silica particles was influenced by the volume ratio of water/soybean oil, the cycle number of the sequential ultrasound irradiation, and the amount of organosilane added to the emulsion. The emulsion was stabilized by Ostwald ripening, as the size distribution at 5/10³ (water/oil = v/v) was a bimodal split between a water droplet size of a few μm and some with a size of a few tens of nm. The most appropriate cycle number was 3 in this system. Further cycling to 5 resulted in a broad and bimodal size distribution of the final particles due to rapid coalescence of water droplets. Subsequent hydrolysis of methylsilyl trichloride consumed water with diminishing large droplets, forming fine and unimodal (0.12 ± 0.02 μm) hollow silica particles. Very fine and uniform-sized hollow particles (0.08 ± 0.01 μm) were successfully produced by decreasing the volume ratio to 1/10³ (water/oil) because of a transparent stable emulsion as a homogeneous template of the hollow structures.

 Received 30th April 2021
 Accepted 23rd June 2021

DOI: 10.1039/d1ra03384k

rsc.li/rsc-advances

1. Introduction

Liquid droplets have received attention in many areas: cosmetic, heat-transportation, drug delivery, food, pharmaceuticals, and material synthesis. The liquid droplets dispersed in emulsion systems are templates for macro/nano spherical capsules, where the interface provides a polymerization field for the formation of hollow spheres on the liquid template.^{1,2} The

liquid droplets vaporized after the deposition, whereas solid spherical templates³ need calcination or dissolution to be removed.^{4,5} The emulsion templates have been employed in the synthesis of hollow nanostructures since 1964, first used by Chang.⁶ The hollow spheres of silica^{7,8} and organosilicas^{9–14} have been studied in inorganic microspheres due to their stability and flexibility in altering surface functionalities. Simple oil-in-water (O/W),^{15–18} water-in-oil (W/O),^{19–22} and double (water-in-oil) in water (W/O/W)^{23–26} emulsion systems have been used to fabricate hollow nano/macrospheres of silica (organosilica), dissolving various building units, such as silica sol (dissolved in a water phase) and silane-coupling agents (in an oil phase). In contrast to a solid-template free method with controlled size (*e.g.*, the Stöber method),²⁷ the procedure, which uses liquid droplets in an emulsion is a way to include chemical substances with varying compositions of liquid droplets, thereby introducing functionalities.^{28–31}

Nanoemulsions with droplet sizes in the order of 100 nm (ref. 32) are useful templates for nanospherical hollow particles because of their kinetic stability, high surface area per unit volume, and optical transparency. Various methods for preparing nanoemulsions include high pressure homogenization,^{33–35} phase inversion temperature and emulsion inversion point,^{36,37} and the bubble bursting method.³⁸ Ultrasound emulsification is also a useful and facile technique for dispersing immiscible

^aDepartment of Materials Chemistry, Faculty of Engineering, Shinshu University, 4-17-1, Wakasato, Nagano 380-8553, Japan. E-mail: tomohiko@shinshu-u.ac.jp; Fax: +81-26-269-5424; Tel: +81-26-269-5414

^bResearch Initiative for Supra-Materials, Shinshu University, 4-17-1, Wakasato, Nagano 380-8553, Japan

† Electronic supplementary information (ESI) available: Particle size distributions of the products obtained after adding 1.9 mmol MTCS to the 0.10 mL water dispersing soybean oil emulsion, which was prepared through the sequential ultrasound irradiation in 1 cycle (Fig. S1), in 3 cycles (Fig. S2), and in 5 cycles (Fig. S3), optical microscope image of mixture of 0.10 mL water with 50 mL soybean oil prepared in 3 cycles of the sequential ultrasound irradiation (Fig. S4), SEM images of the products using W/O emulsion (dispersing 1.0 mL water) prepared in 3 cycles of the sequential ultrasound irradiation (Fig. S5), particle size distributions of the products obtained after adding 9.3 mmol MTCS to the 0.50 mL water (Fig. S6) 18 mmol MTCS to the 0.97 mL water (Fig. S7), 21 mmol MTCS to the 0.97 mL water (Fig. S8), 0.93 mmol MTCS to the 0.05 mL water (Fig. S9), and 0.70 mmol MTCS to the 0.05 mL water (Fig. S10), dispersing soybean oil emulsion, prepared through the sequential ultrasound irradiation in 3 cycles. See DOI: 10.1039/d1ra03384k



water in oil and *vice versa*.³⁹ Emulsion stability is necessary for achieving a uniform droplet size because the interfacial deposition competes against the flocculation and coalescence of the droplets. Additives (*e.g.*, electrolytes, surfactants, and polymers) and oils (due to their viscosity, specific gravity, and dielectric constant) are used to stabilize emulsions. Although surfactants can be used to improve colloidal stability, surfactant-free emulsions^{40,41} eliminate the need for surfactant removal; thus, simplifying the preparation process.

Regulation of droplet size dispersed in the continuous phase is a research area that aims at controlling the particle size. Low-frequency ultrasound emulsification (*e.g.*, high-power homogenizers at ~ 20 kHz and cleaning bath at ~ 40 kHz) destabilizes the oil/water interface by surface vibration and disruption of droplets through cavitation.^{42,43} Kamogawa and coworkers paid attention to the accelerating effect of megasonic ultrasounds on solvent molecules and particulates; this emulsification in surfactant-free O/W system is prevented from damaging the liquid molecules.⁴⁴ Instead of kilohertz ultrasounds, as cavitation rarely occurs in submegasonic-megasonic irradiation, megasonic irradiation leads to the breaking of pre-dispersing droplets at the submicrometer scale. Unimodal size of droplets was achieved in stable emulsion because the resulting small oil droplets were far from re-coalescence,⁴⁴ thus, submegasonic-megasonic irradiation is recognized as an additional processing surfactant-free O/W emulsion. Fine and unimodal droplets have been used to prepare hollow spherical particles based on the sequential ultrasound irradiation.^{45–47}

In contrast to various examples of the O/W mixtures, limited examples were applied to surfactant-free W/O emulsions.⁴⁸ Electrolytes and water-soluble species can be included in the W/O emulsion systems by dissolving them in water droplets, whereas water-insoluble chemicals can be included in oil droplets in the O/W systems.⁴⁹ Efforts to develop hollow-sphere particles in the absence of surfactants in a simple W/O emulsion has been made.^{20,22,50–55} Cyclohexane in the continuous

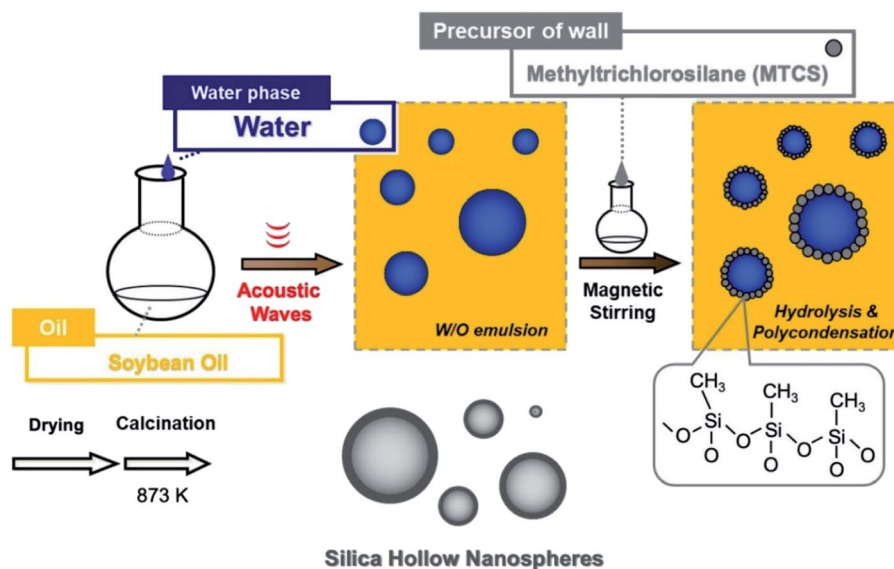
phase resulted in the formation of the most stable emulsion, which is made up of $0.97 \mu\text{m}$ aqueous droplets, and afforded smaller and uniform-sized hollow silica ($0.10 \pm 0.020 \mu\text{m}$), due to dispersed aqueous droplets clusters formed by the breakup of $0.97 \mu\text{m}$ -droplets upon hydrolysis of silicon alkoxide.⁵⁵ We focused on using organosilyl chlorides in a W/O emulsion due to its rapid polymerization compared to that of alkoxides (without an additional catalyst for the facile encapsulation of functional nanoparticles).^{50–54} Thus, polymerization can be used to make functional encapsulated particles, such as magnetic particles^{50,51} and solid-acid catalysts.^{52,53} The microcavity in the hollow spheres is reflected in the final size of the droplets produced by kilohertz ultrasounds, however, the distributions are frequently bimodal in the sizes of final the hollow particles, with particle sizes observed a few tens of nm and a few μm , except for concentrated NaCl aqueous solution dispersed in soybean oil (continuous phase).⁵⁴

To improve the potency of introducing varieties of functionalities in the nanocavity, we apply sequential ultrasound irradiation (28 kHz \rightarrow 200 kHz \rightarrow 950 kHz) to a simple W/O emulsion for producing unimodal (organic)silica nanospherical capsules (Scheme 1). Methyltrichlorosilane (abbreviated to MTCS) was employed in the interfacial deposition to provide hollow particles without additives (*e.g.*, surfactant and encapsulating substance). Here, we discuss how kinetic stability of the emulsion influences the final size distribution of hollow particles: (i) changing the volume ratio of soybean oil/water, (ii) cycle number of sequential ultrasonic irradiation and (iii) amount of MTCS in the mixture of soybean oil with water droplets.

2. Experimental

Reagents and materials

Methyltrichlorosilane (MTCS) was purchased from Shin-Etsu Chemical Co., Ltd. Isooctane (2,2,4-trimethylpentane) and soybean oil were purchased from FUJIFILM Wako Pure Chemical Co., Ltd. These materials were used as received.



Scheme 1 Schematic representation of hollow silica nanocapsules formation using ultrasonically prepared W/O emulsion and hydrolysis/polymerization of methyltrichlorosilane (MTCS).



Preparation of a W/O emulsion

A given volume of water (0.05, 0.10, 0.50, and 0.97 mL: 2.8, 5.7, 28, and 54 mmol) was added to 50 mL of soybean oil in a round bottom flask. After shaking for 10 s at room temperature, the mixture was successively treated in ultrasound baths for 5 min in the order of 28 kHz, 200 kHz, and 950 kHz types. This sequential ultrasound irradiation process was repeated at most 5 times. The colloidal stability of each emulsion was evaluated by recording its turbidity using a UV-Vis spectrophotometer at 700 nm for 4 days (where the optical path length used was 10 mm).

The polymerization of MTCS on the aqueous droplets

A given amount of MTCS (molar ratio of MTCS to water was 1 : 3) dissolved in soybean oil (10 mL) was slowly poured into the freshly prepared W/O emulsion under magnetic stirring (Table 1). The stirring was conducted at room temperature for 3 h for hydrolysis and polymerization of MTCS on the aqueous droplets. Filtration was performed using a conventional suction filtration apparatus fitted with a 0.2 μm -mixed cellulose ester (ADVANTEC) membrane, and then, the isolated solid was washed with isooctane to remove unreacted MTCS. The isolated solid was dried at different temperatures in the order of 323 K and 393 K for 1 day in each, followed by calcination at 873 K in an electronic furnace for 3 h to convert the polymethylsiloxane to silica.

Equipment

The turbidity of the W/O emulsion was monitored by observing changes in the transmission spectra centered at 700 nm using a Shimadzu UV-2450PC spectrophotometer. The viscosity of the emulsion was measured by a tuning fork vibro viscometer (30 Hz, SV-10A, A&D Co., Ltd.). The size distribution of the water droplets was recorded using KEYENCE digital microscope VHX-8000. Scanning electron micrography (SEM) images were captured on a Hitachi SU-8000 field-emission scanning electron microscope. The transmission electron micrography (TEM) images were obtained using a Hitachi High-Tech HD-2300A spherical aberration-corrected scanning transmission electron

microscope (operated at 200 kV). Particle diameters of hollow spheres were determined using the TEM images ($N = 100$).

3. Results and discussion

Cycles of sequential ultrasound irradiation

Sequential ultrasound irradiation (28 kHz \rightarrow 200 kHz \rightarrow 950 kHz) was performed for emulsification of a mixture of 0.10 mL water with 50 mL soybean oil, before the addition of MTCS. A stable opaque suspension was obtained immediately after 28 kHz ultrasonic irradiation. The addition of MTCS to each fresh W/O emulsion resulted in precipitation due to the hydrolysis and condensation of MTCS, forming spherical particles with a partly deformed hollow shape (Fig. 1a).⁵⁴ However, size distribution was bimodal split between particles of a few hundred nm and some with a size of a few tens of nm. In contrast, the sequential ultrasound irradiation of 1 cycle (run 1) led to the appearance of the submicrometer spherical particles (Fig. 1b). This appearance is attributed to the high mechanical effects of the submegasonic irradiation breaking up a large droplet template of water, as observed in another emulsion system.^{44–47} TEM observations show hollow morphology/structure. Repeated sequential ultrasound irradiation for 3 cycles reduced the larger spheres (Fig. 1c: run 2) to make a unimodal size distribution. In Table 1, the mean particle size was 0.12 μm and the standard deviation was 0.02 μm reflecting from the diminishing of the larger particles (maximum diameter was 0.19 μm , which was decreased from that prepared in 1 cycle). However, further cycling of sequential ultrasound irradiation to five (run 3) resulted in broad size distribution (Fig. 1d, increases in the standard deviation and observed maximum diameter). The above-described distributions in size are displayed as histograms in the ESI, Fig. S1–S3.†

Fig. 2a displays the turbidity of W/O emulsion comprising a mixture of 0.10 mL water with 50 mL soybean oil after preparation with the elapsed time. Here, we discussed how the long-term-colloidal stability of W/O emulsion correlates with the size distribution of final particles (Fig. 1). The transmittance of W/O emulsion was lower than 1% for 1 day, independent of the number of operating sequential ultrasound irradiation cycles.

Table 1 Compositions of starting mixture in surfactant-free water-in-soybean oil emulsion and results of the final particle size

Run No.	Cycle	Water ^a			Particle size [μm] ($N = 100$)			
		[mL]	[mmol]	MTCS ^a [mmol]	Mean	S.D. ^b	Maximum	Histogram
1	1	0.10	5.7	1.9	0.13	0.03	0.25	Fig. S1
2	3	0.10	5.7	1.9	0.12	0.02	0.19	Fig. S2
3	5	0.10	5.7	1.9	0.12	0.04	0.35	Fig. S3
4	3	0.50	28	9.3	0.13	0.03	0.25	Fig. S6
5	3	0.97	54	18	0.17	0.08	0.54	Fig. S7
6	3	0.97	54	21	0.13	0.02	0.18	Fig. S8
7	3	0.05	2.8	0.93	0.06	0.01	0.10	Fig. S9
8	3	0.05	2.8	0.70	0.08	0.01	0.12	Fig. S10

^a After a given volume of water was dispersed in 50 mL soybean oil for preparing W/O emulsion, methyltrichlorosilane (MTCS) dissolved in 10 mL soybean oil was added. ^b S.D.: standard deviation.



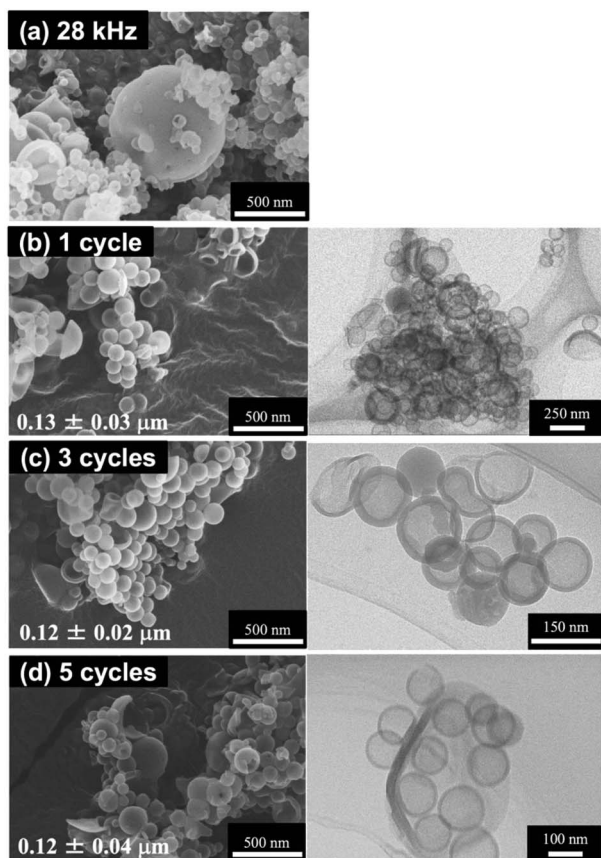


Fig. 1 (left) SEM and (right) TEM images of the products obtained after the addition of 1.9 mmol-methyltrichlorosilane (MTCS) to W/O emulsion including 0.10 mL water: The SEM image shown in part (a) is the emulsion product prepared by irradiating 28 kHz ultrasound. The SEM and TEM images in parts (b), (c), and (d) are of the products through the sequential ultrasound irradiation by 1, 3, and 5 cycles, respectively.

The colloidal stability was enhanced for 3 cycles of the sequential ultrasound irradiation among the tested W/O emulsions. The cycling irradiation through submega-

sonications (200 and 950 kHz) is effective for mechanical break up of large droplets, and elongation of the irradiation would decrease viscosity of water-in-soybean oil mixtures driven by an increase in temperature. In Fig. 2b, the temperature of soybean oil increased with the number of cycles from $T = 286$ K to 299 K, and the viscosity, K (mPa s), decreased according to eqn (1):

$$K = a e^{\left(\frac{b}{T^3}\right)}, \quad (1)$$

where a and b are constants ($a = 8.32 \times 10^{-3}$ and $b = 1.08 \times 10^8$).⁵⁶ Sedimentation of water droplets in W/O emulsion is defined by Stokes equation, eqn (2):

$$u = \frac{r^2(\rho_0 - \rho)g}{18\eta}, \quad (2)$$

where u is the sedimentation rate of water droplets in W/O emulsion, r is the radius of the water droplet, $(\rho_0 - \rho)$ is the density difference between oil continuous phase and water-dispersed phase, η is the viscosity of oil (continuous phase), and g is the gravitational acceleration. Considering a small difference in the mean particle diameter (Table 1), we deduce that the decrease in the viscosity would proceed to coalescence and flocculation of water droplets and that finally yield a broad size distribution. 3 cycle has been adopted as the sequential ultrasound irradiation procedure for preparing W/O emulsion templates because the production of the unimodal size distribution of hollow particles requires good colloidal stability.

Correlation of droplet size with final diameter of silica hollow spheres

A laser diffraction apparatus may be unsuitable for measuring diameters of the aqueous droplets in highly viscous soybean oil-based W/O emulsions due to mixing with air bubbles. Moreover, an optical microscope was employed with thresholding image for the number of 4312 droplets, resulting in a broad range as mean size of 1.8 μm (standard deviation of 1.5 μm) for the

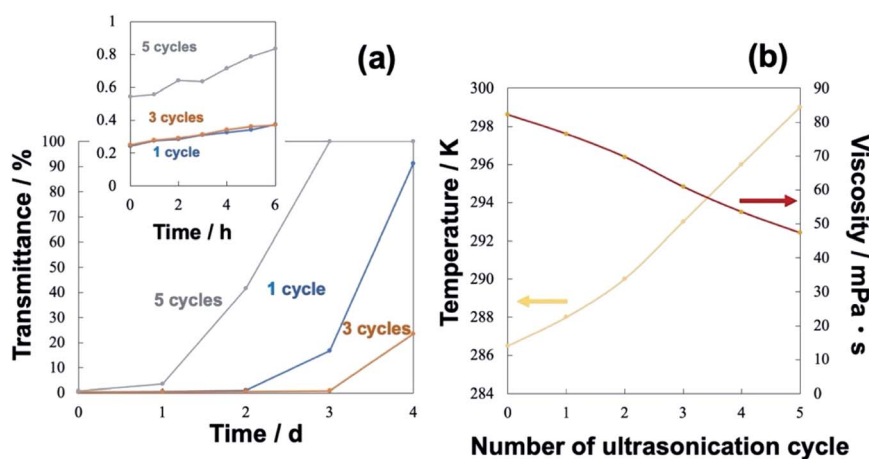


Fig. 2 (a) The time-course profiles of the transmittance ($\lambda = 700$ nm) recorded after the sequential ultrasound irradiation (28 kHz \rightarrow 200 kHz \rightarrow 950 kHz) of 0.10 mL water in 50 mL soybean oil and (b) the changes in temperature and viscosity of soybean oil upon cycling of the sequential ultrasound irradiation.



mixture of 0.10 mL water with 50 mL soybean oil (the optical microscope image is shown in the ESI, Fig. S4†). The colloidal stabilization would be maintained by forming a bimodal size distribution of water droplets *via* Ostwald ripening because of a large population of submicrometer range (approximately 20% around 0.2 μm).^{48,54} Coexisting micrometer-scaled droplets are responsible for turbidity. Although we cannot visualize small droplets of less than 0.2 μm , the final particle size distribution (Fig. 1c: run 2: $0.12 \pm 0.02 \mu\text{m}$) extremely differed from the droplet sizes.

Horikoshi *et al.*⁵⁵ reported that uniform-sized hollow silica ($0.10 \pm 0.020 \mu\text{m}$) was provided using tetraethylorthosilicate from cyclohexane-based W/O emulsion, comprising 0.97 μm -aqueous droplets. They observed dispersing aqueous droplet clusters formed by the breakup of 0.97 μm -droplets upon hydrolysis of tetraethylorthosilicate. In our former case, because the molar ratio of water/MTCS was 3 before the hydrolysis, numerically almost of all water molecules were once consumed through the hydrolysis of MTCS (but the water molecules reform by the polycondensation). Presently, MTCS hydrolyzes and polymerizes without additional catalyst, the droplet refinement by hydrolysis is rapid compared to alkoxides. The formation (polymerization of the hydrolyzed MTCS) of the hollow structures would be followed by the aggregation of water nanodroplets with the hydrolyzed MTCS.

There is no direct relation of the long-term stability over 1 day (Fig. 2) with the controlled final size of hollow structures. When the MTCS addition to the W/O emulsion was postponed to 30 and 60 min after preparing emulsion, large particles (approx. 0.5 μm in diameter) emerged with a broad size distribution, as shown in SEM images (see the ESI, Fig. S5†). Though the emulsion was stabilized over a long period, the diffusion of water molecules between water droplets (Ostwald ripening) initiated after preparing W/O emulsion continued. Therefore, breaking up large droplets by sequential ultrasound irradiation is necessary to produce unimodal hollow silica particles. However, we assumed that MTCS affects restricting the growth of water droplets like an emulsifier. In fabricating unimodal sized-hollow nanospheres, we found that an important aspect is the timing of the MTCS addition after preparing W/O emulsion.

The volume of water droplets in soybean oil (continuous phase)

The variation in the volume of water (dispersed phase) was examined. Even when the volume was increased from 0.10 mL to 0.50 and then, 0.97 mL in 50 mL soybean oil, the mixtures afforded good colloidal stability for a long period because the turbidity of W/O emulsion was within 1% over the 3 d period (Fig. 3a). The turbidity was dropped over 4 d; the measured transmittance $\sim 50\%$ for 0.50 mL water was larger than that (25% in transmittance) for 0.10 mL water. The colloidal stability was high when the water volume was increased to 0.97 mL because of higher turbidity (lower transmittance, $\sim 15\%$). A large volume of water droplets in the oil (continuous phase) contributes to colloidal stability due to an increase in viscosity in some cases.⁵⁷ The viscosity of the mixture, comprising

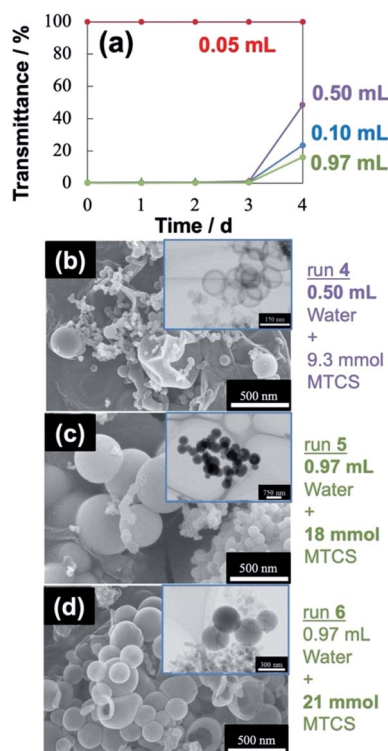


Fig. 3 (a) The time-course profiles of the transmittance ($\lambda = 700 \text{ nm}$) recorded after the sequential ultrasound irradiation (28 kHz \rightarrow 200 kHz \rightarrow 950 kHz) of different volumes of water in 50 mL soybean oil, and the SEM and TEM images of the products obtained by reacting (b) 9.3 mmol, (c) 18 mmol, and (d) 21 mmol methyltrichlorosilane (MTCS). The volume of water was (b) 0.50 mL and (c,d) 0.97 mL.

0.97 mL water and 50 mL soybean oil, was 56.2 mPa s, which is larger than the 0.1 mL water dispersion (48.1 mPa s).

Contrary to enhancing colloidal stability by dispersing 0.97 mL water, the mean size was large in the final particles obtained by MTCS addition (Table 1). In Figs. 3b and 3c, SEM and TEM images display bimodal size distribution in both cases of increasing the water volume to 0.50 mL (run 4: the size distribution is shown in the ESI, Fig. S6†) and to 0.97 mL (run 5: in the ESI, Fig. S7†), respectively. The colloidal stability would be secured by forming a bimodal distribution of water droplets through Ostwald ripening split between water droplets of a few μm and the size lower than a few hundred nm. In the case of using 0.97 mL water, unfortunately, dense (not hollow) particles were observed in the TEM image (Fig. 3c) for smaller particles. This accounted for the remaining micrometer-scaled droplets after the sequential ultrasound irradiation and thus, for the small sum of interface area (or surface area of water droplets in total) for the polymerization of excess amount of hydrolyzed MTCS. When added MTCS was increased from 18 to 21 mmol (run 6), the final particles became smaller and the size distribution becomes narrow (Fig. 3d, $0.13 \pm 0.02 \mu\text{m}$, the size distribution is shown in the ESI, Fig. S8†). The decrease is the result of the breakup of large droplets driven by the hydrolysis of a larger amount of MTCS, however, dense particles were obtained due to excess hydrolyzed MTCS.



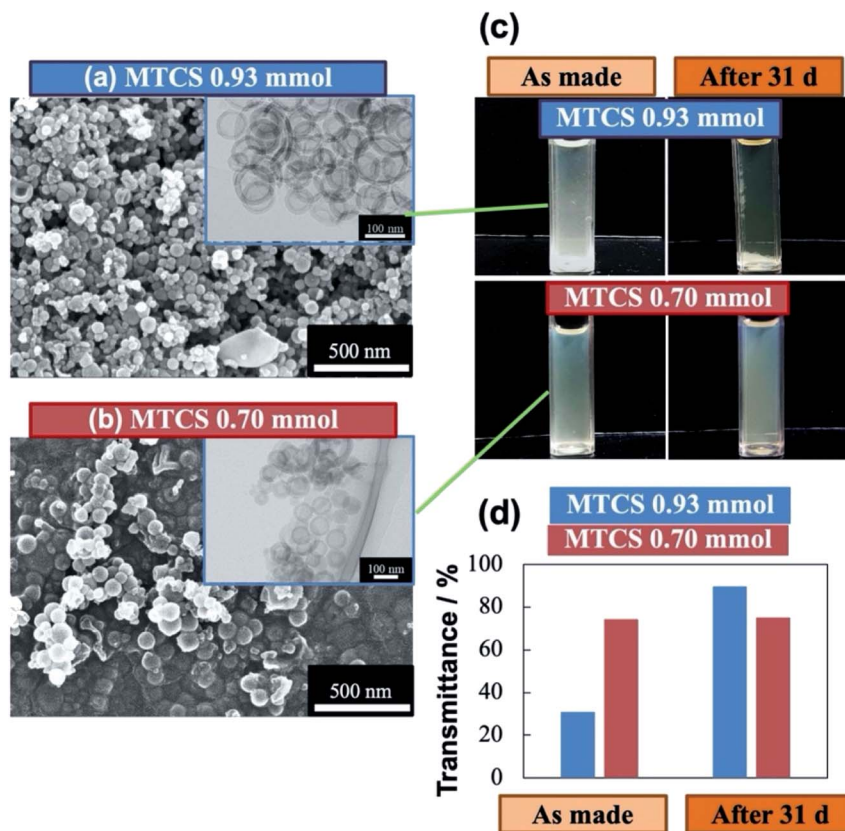


Fig. 4 SEM and TEM images of the products obtained by reacting (a) 0.93 mmol and (b) 0.70 mmol of methyltrichlorosilane (MTCS) in 0.05 mL water dispersed in soybean oil: Photographs (c) and transmittances (d) as-made dispersions after adding MTCS and after 31 days.

When water volume was reduced from 0.10 mL to 0.05 mL, the mixture after the sequential ultrasound irradiation was completely transparent, which was secured for over 4 d (Fig. 3a). The sequential ultrasound irradiation required 3 cycles to be transparent, whereas less than 3 cycles remained opaque. This transparency was indicative of emerging fine water droplets/clusters dispersed in the oil (continuous phase).^{32,58} The final particles obtained by adding 0.93 mmol of MTCS was fine hollow spheres (run 7: the mean diameter of 0.06 μm , the maximum diameter of 0.10 μm) and was indeed monodisperse with a standard deviation of 0.01 μm (Fig. 4a, the size distribution is shown in the ESI, Fig. S9[†]). Therefore, the low fraction of water volume ($1/10^3$) is important in producing (organo)silica nanocapsules under unimodal size control, as well as long-term stabilization of W/O nanoemulsion. Negligible negative effects were obtained by reducing MTCS from 0.93 to 0.70 mmol (run 8) on the size distribution of final particles; the mean diameter of hollow particles was $0.08 \pm 0.01 \mu\text{m}$ (Fig. 4b, the size distribution is shown in the ESI, Fig. S10[†]).

Finally, we examined the long-term dispersion ability of polymerized MTCS using the 0.05 mL water dispersion in soybean oil. The dispersions include water-encapsulated polymethylsiloxane without drying and subsequent calcination at 873 K. Only a slight size reduction was observed upon the calcination, comparing the size distribution in the ESI Figs S9 and S10. In Fig. 4c, photographs were captured just after

preparing W/O emulsion and subsequent addition of 0.70 and 0.93 mmol MTCS, where the calculated concentrations of polymerized MTCS were 0.8 and 1.1 g L^{-1} , respectively. The difference in the concentration reflects the turbidity (transmittance, Fig. 4d); a higher concentration of the MTCS dispersion yielded lower transmittance ($\sim 30\%$) as is prepared. In contrast, the dispersion stability was maintained over 1 month for the lower concentration (0.70 mmol MTCS, 0.8 g L^{-1}); the transmittance (approx. 70%) was constant during the long period due to a negligible gravimetric effect.

4. Conclusions

We have investigated a methodology for regulating the size of nanometer-sized hollow silica sphere particles using a surfactant-free W/O emulsion. The W/O emulsion was prepared *via* sequential ultrasonic irradiation (28 kHz \rightarrow 200 kHz \rightarrow 950 kHz), followed by the interfacial deposition of MTCS. Based on stabilizing emulsion Ostwald ripening, the final structure/morphology of the silica particles was influenced by (i) the volume ratio of water/soybean oil, (ii) cycle number of the sequential ultrasound irradiation, and (iii) amount of MTCS in the emulsion. The following is detailed descriptions of these points.

(i) There are remains of micrometer-sized droplets at a high volume ratio of water/soybean oil (more than $5.0/10^3$) even after



submegasonic irradiation. The subsequent hydrolysis of MTCS consumed water dispersing soybean oil at $5/10^3$ (water/oil) to diminish the micrometer-sized droplets, resulting in uniform-sized nanospherical hollow silica particles ($0.12 \pm 0.02 \mu\text{m}$). A decrease in the ratio to $1/10^3$ (water/oil) afforded a transparent stable emulsion and uniform-sized hollow particles ($0.08 \pm 0.01 \mu\text{m}$).

(ii) The most appropriate cycle number was 3 in this system. Further cycling to 5 resulted in a broad and bimodal size distribution of final particles due to rapid coalescence of water droplets that were directly influenced by decreasing viscosity (increasing temperature).

(iii) Typically, we examined using the molar MTCS/water ratio of 1 : 3 because water added was numerically consumed by hydrolysis of MTCS. An excess amount of MTCS added reduced the final size of particles. Thus, MTCS affects breaking water droplets in the hydrolysis and restricting the growth of water droplets like an emulsifier. For providing unimodal sized-hollow nanospheres, MTCS should be added after preparing W/O emulsion.

Fine and uniform-sized droplets that formed in the low volume ratio of $1/10^3$ (water/oil) manifested as a template for the final nanospherical silica capsules produced by the interfacial condensation of MTCS. These findings should gain insight into the synthetic strategy of unimodal nanocapsules using various W/O emulsion systems in the presence of emulsifiers and electrolytes in the aqueous phase.

Conflicts of interest

There are no conflicts of interest to declare.

Acknowledgements

This work was supported by JSPS KAKENHI (Grant-in-Aid for Scientific Research), Grant number of 20K05661.

References

- 1 X. Wang, J. Feng, Y. Bai, Q. Zhang and Y. Yin, *Chem. Rev.*, 2016, **116**, 10983–11060.
- 2 K. Piradashvili, E. M. Alexandrino, F. R. Wurm and K. Landfester, *Chem. Rev.*, 2016, **116**, 2141–2169.
- 3 F. Caruso, R. A. Caruso and H. Mohwald, *Science*, 1998, **282**, 1111–1114.
- 4 X. W. Lou, L. A. Archer and Z. Yang, *Adv. Mater.*, 2008, **20**, 3987–4019.
- 5 G. Prieto, H. Tüysüz, N. Duyckaerts, J. Knossalla, G.-H. Wang and F. Schüth, *Chem. Rev.*, 2016, **116**, 14056–14119.
- 6 T. M. Chang, *Science*, 1964, **146**, 524–525.
- 7 J. Hu, M. Chen, X. Fang and L. Wu, *Chem. Soc. Rev.*, 2011, **40**, 5472–5491.
- 8 K. Ariga, Q. Ji, G. J. Richards and J. P. Hill, *Soft Matter*, 2012, **10**, 387–412.
- 9 H. Djojoputro, X. F. Zhou, S. Z. Qiao, L. Z. Wang, C. Z. Yu and G. Q. Lu, *J. Am. Chem. Soc.*, 2006, **128**, 6320–6321.
- 10 L. Beaudet, R. Pitre, L. Robillard and L. Mercier, *Chem. Mater.*, 2009, **21**, 5349–5357.
- 11 J. Liu, S. Bai, H. Zhong, C. Li and Q. Yang, *J. Phys. Chem. C*, 2010, **114**, 953–961.
- 12 M. Quesada, C. Muniesa and P. Botella, *Chem. Mater.*, 2013, **25**, 2597–2602.
- 13 Y. Maki, Y. Ide and T. Okada, *Chem. Eng. J.*, 2016, **299**, 367–372.
- 14 B. P. Binks, *Langmuir*, 2017, **33**, 6947–6963.
- 15 C. I. Zoldesi and A. Imhof, *Adv. Mater.*, 2005, **17**, 924–928.
- 16 C. I. Zoldesi, C. A. van Walree and A. Imhof, *Langmuir*, 2006, **22**, 4343–4352.
- 17 C. I. Zoldesi, P. Steegstra and A. Imhof, *J. Colloid Interface Sci.*, 2007, **308**, 121–129.
- 18 S.-H. Wu, Y. Hung and C.-Y. Mou, *Chem. Mater.*, 2013, **25**, 352–364.
- 19 M. Jafellici, M. R. Davolos Jr, F. J. Santos and S. J. Andrade, *J. Non-Cryst. Solids*, 1999, **247**, 98–102.
- 20 S. Mishima, M. Kawamura, S. Matsukawa and T. Nakajima, *Chem. Lett.*, 2002, 1092–1093.
- 21 M. O'Sullivan and B. Vincent, *J. Colloid Interface Sci.*, 2010, **343**, 31–35.
- 22 S. Mishima, T. Okada, T. Sakai, R. Kiyono and T. Haeiwa, *Polym. J.*, 2015, **47**, 449–455.
- 23 M. Fujiwara, K. Shiokawa, Y. Tanaka and Y. Nakahara, *Chem. Mater.*, 2004, **16**, 5420–5426.
- 24 M. Fujiwara, K. Shiokawa, I. Sakakura and Y. Nakahara, *Langmuir*, 2010, **26**, 6561–6567.
- 25 B. J. Sun, H. C. Shum, C. Holtze and D. A. Weitz, *ACS Appl. Mater. Interfaces*, 2010, **2**, 3411–3416.
- 26 Y. Nonomura, N. Kobayashi and N. Nakagawa, *Langmuir*, 2011, **27**, 4557–4562.
- 27 Y. Du, L. E. Luna, W. S. Tan, M. F. Rubner and R. E. Cohen, *ACS Nano*, 2010, **4**, 4308–4316.
- 28 K. Piradashvili, E. M. Alexandrino, F. R. Wurm and K. Landfester, *Chem. Rev.*, 2016, **116**, 2141–2169.
- 29 C. B. Kim, N.-H. You and M. Goh, *RSC Adv.*, 2018, **8**, 9480–9486.
- 30 W. Wichaita, D. Pollanich, P. Tangboriboonrat, *et al.*, *Ing. Eng. Chem. Res.*, 2019, **58**, 20880–20901.
- 31 Y. F. Zhu, J. Shi, W. Shen, X. Dong, J. Feng, M. Ruan and Y. Li, *Angew. Chem., Int. Ed.*, 2005, **44**, 5083–5087.
- 32 A. Gupta, H. B. Eral, T. A. Hatton and P. S. Doyle, *Soft Matter*, 2016, **12**, 2826–2841.
- 33 T. Tadros, P. Izquierdo, J. Esquena and C. Solans, *Adv. Colloid Interface Sci.*, 2004, **108**, 303–318.
- 34 C. Solans, P. Izquierdo, J. Nolla, N. Azemar and M. J. Garcia-Celma, *Curr. Opin. Colloid Interface Sci.*, 2005, **10**, 102–110.
- 35 C. Qian and D. J. McClements, *Food Hydrocoll.*, 2011, **25**, 1000–1008.
- 36 P. Izquierdo, J. Esquena, F. Tadros, Th. C. Dederen, M. J. Garcia, N. Azemar and C. Solans, *Langmuir*, 2002, **18**, 26–30.
- 37 J. Rao and D. J. McClements, *J. Agric. Food Chem.*, 2010, **58**, 7059–7066.



- 38 J. Feng, M. Roche, D. Vigolo, L. N. Arnaudov, S. D. Stoyanov, T. D. Gurkov, G. G. Tsutsumanova and H. A. Stone, *Nat. Phys.*, 2014, **10**, 606–612.
- 39 S. M. M. Modarres-Gheisari, R. Gavagsaz-Ghoachani, M. Malaki, P. Safapour and M. Zandi, *Ultrason. Sonochem.*, 2019, **52**, 88–105.
- 40 T. Sakai, *Curr. Opin. Colloid Interface Sci.*, 2008, **13**, 228–235.
- 41 S. W. Kim, H. G. Cho and C. R. Park, *Langmuir*, 2009, **25**, 9030–9036.
- 42 M. K. Li and H. S. Fogler, *J. Fluid Mech.*, 1978, **88**, 499–512.
- 43 M. K. Li and H. S. Fogler, *J. Fluid Mech.*, 1978, **88**, 513–528.
- 44 K. Kamogawa, G. Okudaira, M. Matsumoto, T. Sakai, H. Sakai and M. Abe, *Langmuir*, 2004, **20**, 2043–2047.
- 45 K. Nakabayashi, F. Amemiya, T. Fuchigami, K. Machida, S. Takeda, K. Tamamitsu and M. Atobe, *Chem. Commun.*, 2011, **47**, 5765–5767.
- 46 K. Nakabayashi, M. Kojima, S. Inagi, Y. Hirai and M. Atobe, *ACS Macro Lett.*, 2013, **2**, 482–484.
- 47 M. Koshino, Y. Shiraiishi and M. Atobe, *Ultrason. Sonochem.*, 2019, **54**, 250–255.
- 48 T. Sakai and T. Oishi, *J. Taiwan Inst. Chem. Eng.*, 2018, **92**, 123–128.
- 49 Y.-S. Lin, S.-H. Wu, C.-T. Tseng, Y. Hung, C. Chang and C.-Y. Mou, *Chem. Commun.*, 2009, 3542–3544.
- 50 T. Okada, Y. Takeda, N. Watanabe, T. Haeiwa, T. Sakai and S. Mishima, *J. Mater. Chem. A*, 2014, **2**, 5751–5758.
- 51 T. Okada, S. Ozono, M. Okamoto, Y. Takeda, H. M. Minamisawa, T. Haeiwa, T. Sakai and S. Mishima, *Ind. Eng. Chem. Res.*, 2014, **53**, 8759–8765.
- 52 T. Okada, S. Mishima and S. Yoshihara, *Chem. Lett.*, 2009, **38**, 32–33.
- 53 T. Okada, K. Miyamoto, T. Sakai and S. Mishima, *ACS Catal.*, 2014, **4**, 73–78.
- 54 T. Okada and T. Koide, *Langmuir*, 2018, **34**, 9500–9506.
- 55 S. Horikoshi, Y. Akao, T. Ogura, H. Sakai, M. Abe and N. Serpone, *Colloids Surf., A*, 2010, **372**, 55–60.
- 56 K. Kubota, S. Kurisu, K. Suzuki, T. Matsumoto and H. Hosaka, *Nippon Shokuhin Kogyo Gakkaishi*, 1982, **29**, 195–201.
- 57 F. Y. Ushikubo and R. L. Cunha, *Food Hydrocoll.*, 2014, **34**, 145–153.
- 58 D. J. McClements, *Soft Matter*, 2012, **8**, 1719–1729.

